An ANN-based Power System Emergency Control Scheme in the Presence of High Wind Power Penetration

Bevrani H, Tikdari A. G

Published (to be published) in: ***Springer***

publication date: **2010**

Citation format for published version:

Bevrani H, Tikdari A. G (2010) An ANN-based Power System Emergency Control Scheme in the Presence of High Wind Power Penetration. in Wind Power Systems: Applications of Computational Intelligence, pp. 215-254, L. F. Wang, C. Singh, and A. Kusiak (Eds), Springer Book Series on Green Energy and Technology, Springer-Verlag, Heidelberg.

An ANN-Based Power System Emergency Control Scheme in the Presence of High Wind Power Penetration

Bevrani H. and Tikdari A.G.

Re-evaluation of emergency control and protection schemes for distribution and transmission networks are one of the main problems posed by wind turbines in power systems. Change of operational conditions and dynamic characteristics influence the requirements to control and protection parameters.

Introducing a significant wind power into power systems leads to new undesirable oscillations. The local and inter-modal oscillations during large disturbances can cause frequency and voltage relays to measure a quantity at a location that is different to the actual underlying system voltage and frequency gradient. From an operational point of view, this issue is important for those networks that use the protective voltage and frequency relays to re-evaluate their tuning strategies.

In this chapter, an overview of the key issues in the use of high wind power penetration in power system emergency control is presented. The impact of wind power fluctuation on system frequency, voltage and frequency gradient is analyzed, the need for the revising of tuning strategies for frequency protective relays, automatic under-frequency load shedding (UFLS) and under-voltage load shedding (UFLS) relays are also emphasized.

In the present chapter, necessity of considering both system frequency and voltage indices to design an effective power system emergency control plan is shown. Then, an intelligent artificial neural network (ANN) based emergency control scheme considering the dynamic impacts of wind turbines is proposed. In the developed algorithm, following an event, the related contingency is determined by an appropriate ANN using the online measured tie-line powers. A suitable set of voltage sensitivity indices based on a comprehensive voltage stability analysis in the presence of the wind turbines is proposed. Another intelligent ANN is used to

Bevrani H. · Tikdari A.G.
Department of Electrical and Computer Engineering,
University of Kurdistan, Sanandaj, PO Box 416, Kurdistan, Iran

L. Wang et al. (Eds): *Wind Power Systems*, Green Energy and Technology, pp. 215–254.
springerlink.com

examine the stability margin by estimating the system power-voltage (P-V) curves. Finally, the system frequency gradient, voltage sensitivity indices and stability information are properly used by an effective load shedding algorithm. The proposed emergency control scheme and discussions are supplemented by computer nonlinear simulations on the IEEE 9-bus test system.

1 Introduction

To prevent power system blackout following a severe contingency, the emergency control actions are needed. There are few reports on the role of distributed wind turbines in emergency conditions. Frequency and voltage are more frequent decision tools in the emergency control strategies. Interconnection of wind turbines into power system significantly affects the frequency and voltage behavior following the contingencies [2, 7, 11, 12, 16, 21, 23, 36, 42]. Therefore, emergency control schemes may need a revision in the presence of a high penetration wind turbines.

Studying of wind generation impacts on the parameters that used in the emergency control actions make them more useful for the future of the power system that are moving to the systems with high wind power penetration [32].

Annually, many contingencies occur in the real-world power systems, but only some of them lead to the blackout [43]. Identifying the severe contingencies and making adequate analysis help the power system organizer to adjust the emergency control parameters, effectively.

Serious load generation imbalance which is usually the result of a severe contingency may lead the system to the cascading failures and blackout. Engaging the spinning reserve and starting up the non-spinning hydro generators and also, generation re-dispatching may be used to compensate the load generation unbalance [25, 43]. However, even in a power system these services exist, they may be not fast enough to supply the loads rapidly following a large disturbance. Load shedding is a well-known emergency control scheme used to curtail a part of system load in an acceptable time duration. The load shedding algorithms are implemented to shed the loads before loss of remained generation [2, 27].

A variety of studies are recommended to analyze the protection-based penetration limits with consideration of the wind turbine capacity, location and technology. The studies aid in determining mitigation strategies to increase the protection based penetration limit. The loss of coordination, de-sensitization, nuisance fuse blowing, bidirectional relay requirements and overvoltage, should be studied in order to arrive at the penetration limits of wind power in an existing distribution system [2].

The effect of adding wind power units to distribution feeder can produce blind zones for protection devices or upset the coordination between two (or more) protective devices and should be studied carefully [7]. In normal operation, protection devices are coordinated such that the primary protection operates before the backup can take action. Interconnecting distributed wind turbines increases the short circuit level. Depending on the original protection coordination settings along with the size, location and type of the units, uncoordinated situations may be found.

In these situations, the backup operates before the primary, which results in nuisance tripping to some of the loads.

In response to the existing control and coordination challenges, this chapter presents a new intelligent based emergency control scheme that could be more useful for the actual power systems and will be suitable for the power system in the presence of high wind power penetration. Artificial neural networks are effectively used to identify severe faults (contingencies) and estimate the system security level by predicting the post-fault stability margin. Finally, the result is used to run an appropriate load shedding algorithm.

This chapter is organized as follows: in Section 2, the impacts of the wind turbines on the system voltage, frequency, and the rate of frequency change are illustrated. The using of initial frequency gradient in the presence of wind turbines is emphasized. It is shown that simultaneous using of voltage and frequency is required to design an effective load shedding scheme.

Contingency analysis is presented in Section 3. The contingency ranking methods are briefly introduced and some points are suggested to construct a more suitable analysis technique in emergency conditions. The continuation power flow (CPF) which is a common tool to derive the P-V curves is reviewed, and a simple method to obtain the system P-V curves for the suddenly load increasing, corresponds to the emergency conditions, is presented. The P-V curves derived by this method are carefully studied in the power systems with wind turbines for a wide range of load/generation outage.

An overall view of the developed intelligent based emergency control scheme is given in Section 4. In Section 5, a new load shedding algorithm based on the system voltage and frequency is proposed, and its advantages are clarified (in comparison of conventional load shedding plans). To achieve a robust and fast load shedding scheme, appropriate ANNs are suggested for predicting the contingencies and estimating the P-V curves. The proposed analysis and synthesis methodologies are supplemented by adequate nonlinear simulation on the IEEE 9-bus test system.

2 Wind Power Penetration

Increasing the penetration of wind turbine generators (WTGs) in the power system may affects the security/stability limits, frequency, voltage and dynamic behavior of a power system [11, 12, 16, 21, 36, 42]. The WTGs commonly use the induction generators to convert the wind energy into electrical energy [16, 21]. The induction generators are reactive power consumer. Therefore, the voltage of system would be affected in the presence of wind turbines especially in the case of fixed-speed type of WTGs [21]. The wind turbines impacts on the power system frequency and voltage have been studied in many research works [2, 7, 11, 12, 16, 21, 23, 32, 42]. Power system frequency response model in the presence of high WTG penetration, frequency control issue, a survey and some new perspectives are addressed in [2, 7]. In [21], the effects of the doubly-fed induction generator (DFIG) and induction generator (IG) type of WTGs on the voltage transient behavior are explained and the disadvantages of the IG type are shown. Frequency

nadir in the presence of different type of the WTGs has been compared and it is shown in [12, 16]. The load ability of various types of WTGs is compared in [42], and it is shown that the DFIG has larger load ability than IGs.

2.1 Test System

For the sake of dynamic simulations and to describe/examine the proposed methodology, the IEEE nine-bus power system is considered as a test system. A single line diagram for the test system is shown in Fig. 1. As shown, two wind farms are added in buses 5 and 9. Simulation data and system parameters are given in Appendix (Tables 3 to 6).

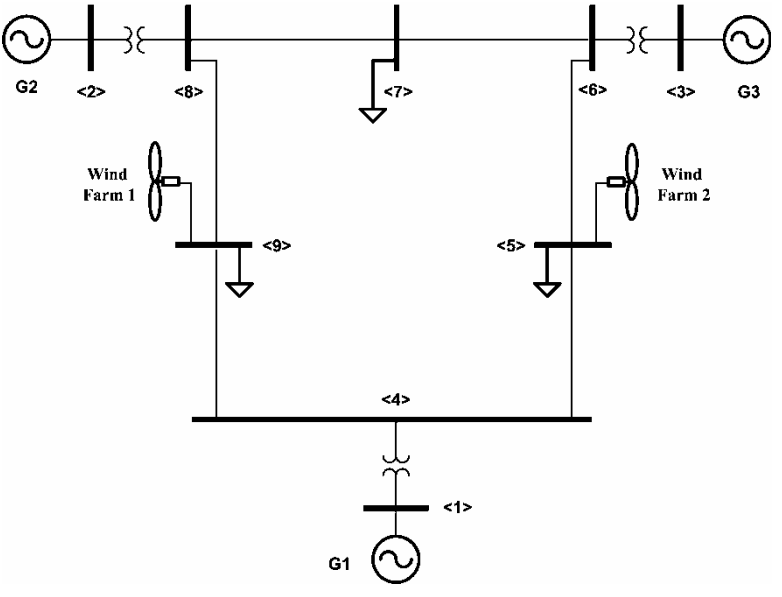

Fig. 1. Nine-bus test system including two wind farms

2.2 Impacts on Voltage Profile

Some reports have addressed the impacts of various WTGs technologies on the voltage deviation following a contingency event, and have analyzed their influences on the transient voltage stability [21, 23].

Fig. 2 shows the voltage response at bus 5 of the test system after tripping of generator G2 (the largest generator) for the following cases: without wind turbine, with 10% DFIG penetration, with 10% IG type penetration, and with 10% IG type wind turbine compensated with a static compensator (STATCOM). As shown, the voltage deviation is significantly affected by integration of wind turbines into the power system. All of them are unstable cases. To protect system against blackout

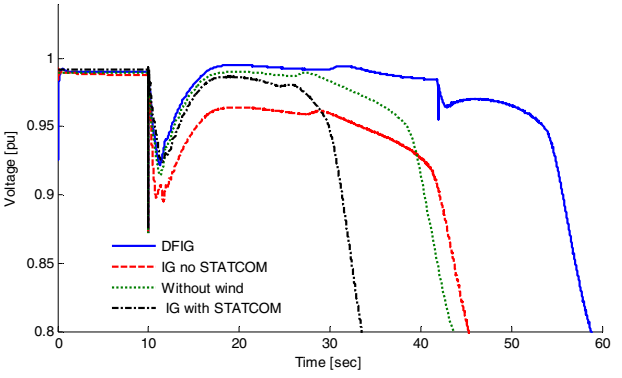

(a)

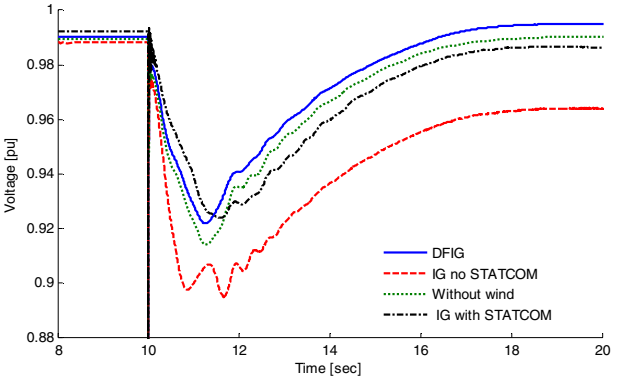

(b)

Fig. 2. Voltage deviation at bus 5 following loss of G2; figure (b) shows a zoomed view around 10s

in these situations, using a load shedding scheme that should be applied at the first few seconds is necessary. Fig. 2 b shows the zoomed view of Fig. 2 a around 10s.

The performed simulation illustrates that the DFIG and IG plus STATCOM represent a better post-contingency performance. But the system performance for the IG type without any reactive support is worse than them under the same test scenario. Absorbing of large amount of grid reactive power by IG wind turbines in the voltage dip cases, can be considered as a reason to present the mentioned behavior [20, 42]. The STATCOM can compensate the reactive power absorption and removes the voltage decline problem. The DFIG type is capable to regulate the power factor by either consuming or producing reactive power [16].

The P-V plot can be considered as a suitable tool to analyze the voltage stability of a power system in the presence of wind turbines. Fig. 3 illustrates the effects of the different wind turbine technologies on the P-V curve for bus 5 of the test system. All of the curves are derived by a slow rate of load admittance change at bus 5. As shown in

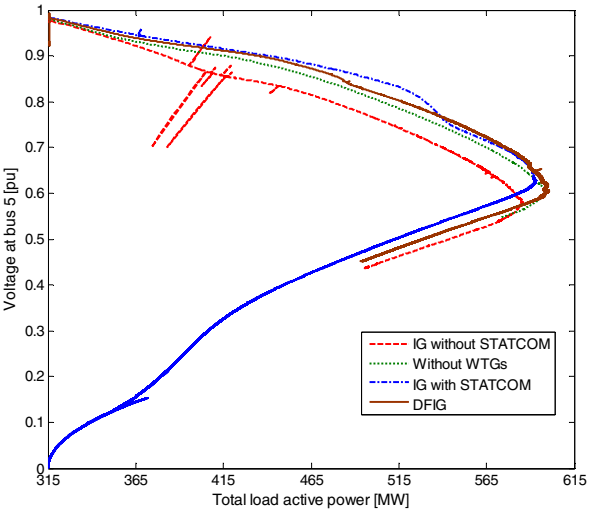

Fig. 3. Comparing the P-V curves in the presence of different type of wind turbine technologies and without WTGs

this figure, the DFIG type of WTG improves the P-V curve and represents a better stability margin for the system. On the other hand, when the IG type is used without any reactive power compensation device, the stability margin decreased, significantly. Since, the STATCOM can compensate the reactive power, in the case of using the IG type equipped with STATCOM, the voltage has been improved.

However, by increasing the power demand, the operating point reaches a point that STATCOM is not able to compensate the reactive power demand for the induction generator more, and the reactive power will be absorbed from the network. Therefore, the P-V curve cannot reach its expected nose and the stability margin to be less than the expected value.

When a generator/line outage takes place, the voltage starts to deviate as shown in Fig. 2. In Section 1.4.2, it will be illustrated that the P-V characteristic is significantly affected by changing the network topology. Therefore, to determine the new power system operating point following a contingency (on the related P-V curve), the post-contingency P-V curve for the test system (considering the network topology changes) to be needed.

2.3 Impacts on System Frequency

Following a large generation loss disturbance, the system frequency may drop quickly if the remaining generation no longer matches the load demand [2, 3]. Some parameters such as power system reserve and inertia constant are influenced by interconnecting the WTGs on the power system. Therefore, the frequency deviation

will be affected in the presence of the WTGs [2, 3, 7, 16]. Fig. 4a shows the frequency response of the IEEE 9-bus test system, following loss of G2 at 10s. This simulation is done for the four cases: without WTG, with DFIG type, with IG type, and with IG type equipped by STATCOM. The initial rate of frequency change for some test scenarios is shown in Fig. 4b. The simulation results show that immediately following a contingency, the frequency behavior of the system in the presence of IG type of WTGs is better than DFIGs. The frequency decline and initial rate of frequency change in the presence of IGs is smaller than the DFIGs case. Because of their structure, IGs add more inertial response to the power system than DFIGs. It is the reason of different frequency behavior illustrated in the Fig. 4.

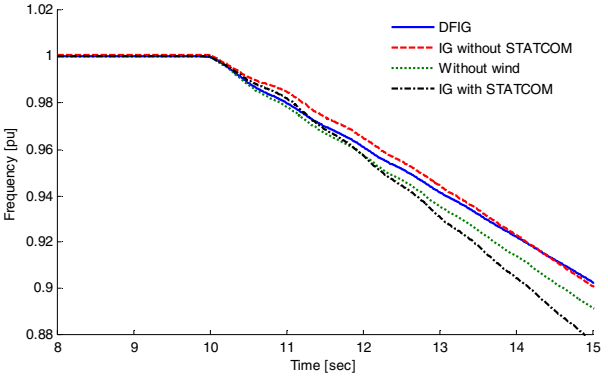

(a)

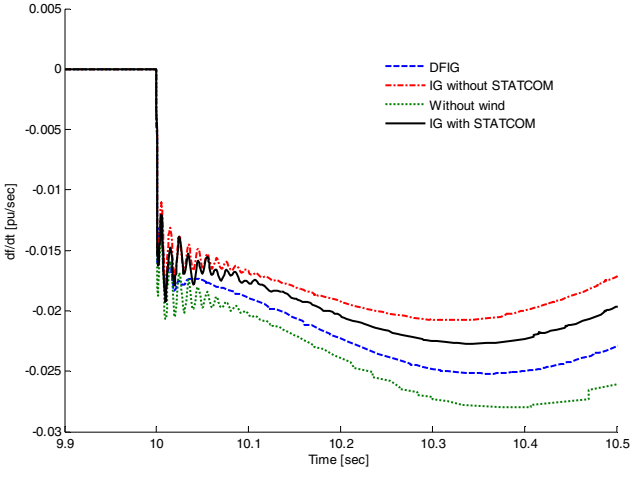

(b)

Fig. 4. System response following G2 outage with and without WTGs (DFIG, IG, and IG equipped with STATCOM); a) frequency deviation, b) rate of frequency change

The initial rate of frequency change is in use as an additional control variable in the recent introduced emergency control algorithms [2, 3, 4, 5, 6, 7, 13]. The initial frequency gradient is proportional to the amount of power imbalance [2]. Therefore, it can be used to determine the amount of load to be shed at the first step of load shedding algorithms. Fig. 2 illustrates that the post contingency voltage behavior in the presence of IG type WTG without STATCOM is the worst case. But, the magnitude of the frequency gradient in this case is the smallest one (Fig. 4b).

Fig. 5 illustrates the simulation results for G1 outage test scenario. The above phenomenon is also exists in this case. The magnitude of frequency gradient in the case of IG with STATCOM is larger than the other cases, while voltage behavior in this case is the best one. On the other hand, voltage deviation in the case of IG without STATCOM is the worst case, while it cannot be justified from the frequency gradient.

This phenomenon indicates that using initial rate of frequency change for the power system emergency control in the presence of wind turbines needs to be revised. Since, in the presence of WTGs, the undesirable oscillations are added to the frequency deviation, the measuring of frequency gradient introduces another difficulty to achieve this variable in emergency control strategies. This issue encourages power design engineers to use $\Delta f/\Delta t$ instead of df/dt [3, 7]. Furthermore, as it is studied in the Section 1.5, voltage and frequency behavior does not address the same results about contingency conditions. This phenomenon is encourages us to re-evaluate the emergency control schemes for the future of the power systems which are integrated with high wind power penetration.

3 Contingency Analysis

A contingency can be created by a three phase fault in a transmission line, a bus bar fault near a generator, etc. These faults are generally eliminated during an acceptable clearing time. But, the consequence protection actions may trip a generator, or curtail a line.

In many cases, generation loss and line outage have a serious impact on the power system performance, and even stability. A major load generation imbalance, line overload and voltage problem may lead the system to a blackout. Identifying the severe contingencies in a power system, performing comprehensive analysis to predict the post contingency conditions and preparing appropriate preventive actions are necessary to design an effective emergency control scheme. This chapter is focused on the major contingencies, and presents a fast, flexible and accurate new algorithm for power system control in emergency conditions.

Contingency screening is a suitable method to rank all contingencies based on their severity and post contingency effects on the power system operating conditions. There are many reports that introduce different algorithms and indices to rank the contingencies [1, 8, 10, 22, 34, 40]. In a contingency analysis, all of possible outages should be simulated and the post contingency conditions should be evaluated [10]. In practice, insist of nonlinear simulation, the contingency analysis problem is generally done in a static environment by considering the steady state operating conditions.

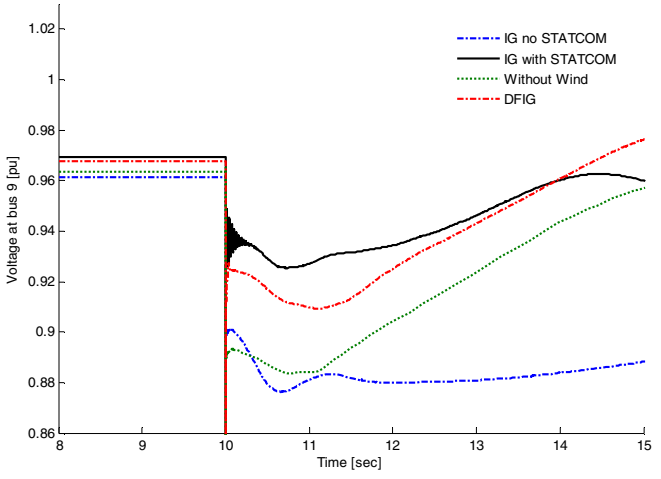

(a)

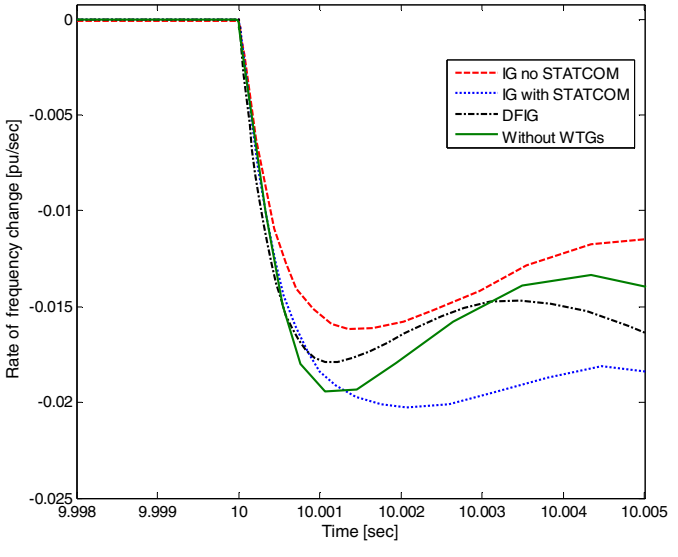

(b)

Fig. 5. System response following G1 outage with and without WTGs (DFIG, IG, and IG equipped with STATCOM); a) voltage deviation, b) initial rate of frequency change

The indices that used to measure the severity of the contingencies are divided into two general groups: the first group is based on the distance to collapse parameter or the magnitude of the stability margins. The second group of indices is based on the steady state parameter violations such as voltage violation and tie-line over loading.

The stability margins could be easily calculated by using P-V curves, Q-V characteristic [1, 22], or studying on the eigen-values of the Jacobin matrix [9]. Ref. [16] introduces some criteria to calculate the stability margin and also performs a direction for load variation at different buses to determine the minimum stability margin or minimum load-ability of system.

Some performance indices are used in above second group. Two typical indices are defined as follows:

$$PI_v = \sum_{\substack{i=1, \\ V^i > V_{max}}}^{N} \left| \frac{V_{max} - V^i}{V_{max}} \right| + \sum_{\substack{i=1, \\ V^i < V_{min}}}^{N} \left| \frac{V_{min} - V^i}{V_{min}} \right| \tag{1}$$

$$PI_p = \sum_{\substack{j=1 \\ |P^i| > P^i_{limit}}}^{L} \left| \frac{P^i}{P^i_{limit}} \right| \tag{2}$$

Here, PI_v and PI_p are the performance indices based on the voltage violations and line overloading, respectively. The V^i, P^i, V_{min}, V_{max}, and P^i_{limit} are post-contingency voltage magnitude at bus *i*, post-contingency of active power line *i*, the allowable voltage magnitude limits, and the maximum transmission capacity of line *i*, respectively. Eq. (1) shows that, wherever the voltage deviations in a contingency violate the specified limits, the performance index of that contingency to be increased. This concept is also used for line over loading in Eq. (2) [10, 34, 40].

Some methods have been introduced for the online and fast contingency ranking [17, 40]. These methods could be more useful in uncertain conditions; such as in a restructured environment, in the presence of high penetration of renewable sources [18], and in a condition that the operating point of the system is unpredictable. The ANNs, fuzzy logic, and other artificial intelligence methods have been widely used in contingency ranking for different purposes such as online ranking [17], and combination of different performance indices [19].

In the proposed emergency control strategy in the present chapter, the contingency ranking step is used. Following, some important points are expanded using a comprehensive simulation on the test system to achieve a more efficient contingency ranking algorithm which is used in the proposed emergency control scheme.

In an emergency condition caused by a serious fault such as the generation outage, a load generation imbalance will be created. The frequency decline and droop characteristic of generator units in a power system lead to increase the unit outputs. It should be considered that in a generation loss case, all remained generator units initially response to the event.

Usually, in steady state analysis and classical AC/DC power flow computation following a generation loss, only the output of the slack generator will be changed. But according to the reality, dividing the output of a tripped generator (in a pre-contingency condition) between the remained units via specific weights on their droop characteristics is more reasonable. A simple method to determine a new operating point following a fault is given in [41].

As mentioned above, a contingency analysis methodology without considering a slack unit could be more useful. Here, also to determine new operating point after a generator outage, the amount of generation loss is divided between all operating units. Then, the power flow calculations will be done, and the performance indices are extracted. Although, this method is not so accurate, it gives an acceptable approximation.

Some nonlinear simulations for a wide range of contingencies in a dynamic environment are performed. Fig. 6 shows the results of the contingency analysis on the IEEE 9-bus test system. Figs. 6a and 6b show the performance indices for the generator outage cases. These figures show the risk of losing of each generator in the nine-bus test system is relatively high. Since, the given power system is small and each generator supplies a considerable portion of load, the above results seems to be reasonable. Figs. 6c and 6d show the performance indices for the line outage cases. For the present example, it is denoted that the loss of lines 7-8, 8-9 and 9-4 show more undesirable post-contingency conditions.

Figs. 7, 8, and 9 confirm the above results, in time-domain responses. Fig. 7 shows the voltage of the weakest bus (bus 9), following various contingencies. Considering Fig. 7 and Figs. 6b and 6d illustrate that the outage of G1 and line 9-4 are significantly degrade the overall system performance. Fig. 6b denotes that the loss of G2 and G3 does not show a serious impact on the bus voltage.

As shown in Fig. 7, the voltage instability starts about 25 seconds after outage of G2 and G3. While, Fig 8 shows the system frequency rapidly falls, immediately after the same event. Therefore, for the present test scenario, system frequency can be considered as a more suitable (than voltage) index to detect the system

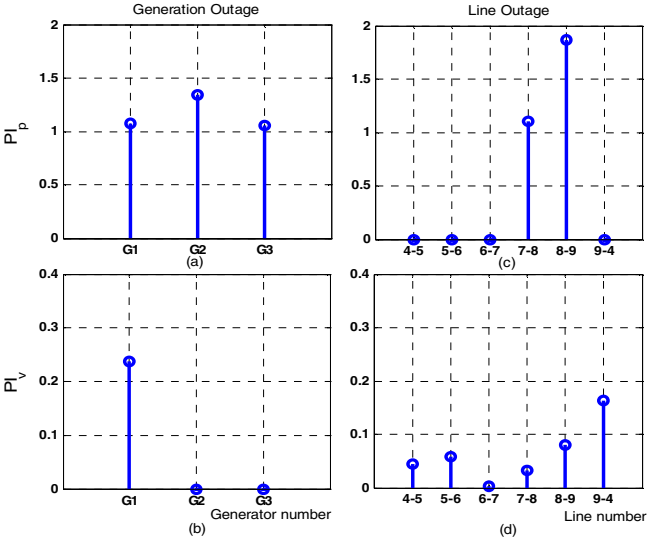

Fig. 6. Performance indices in different contingencies

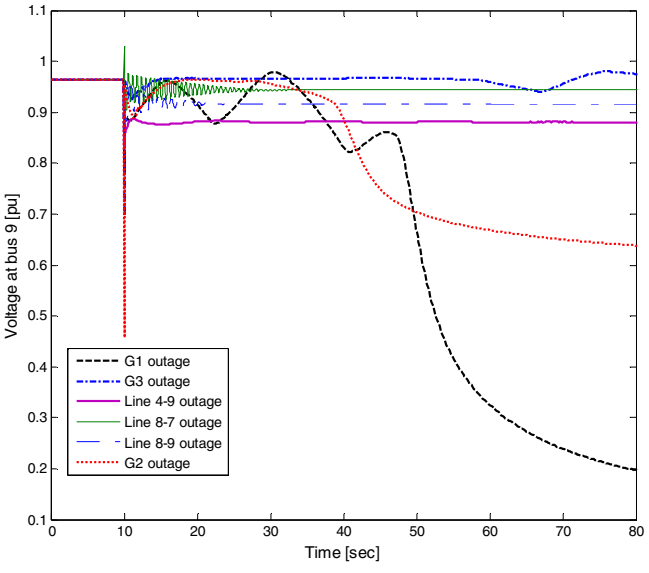

Fig. 7. Weakest bus voltage in different contingencies

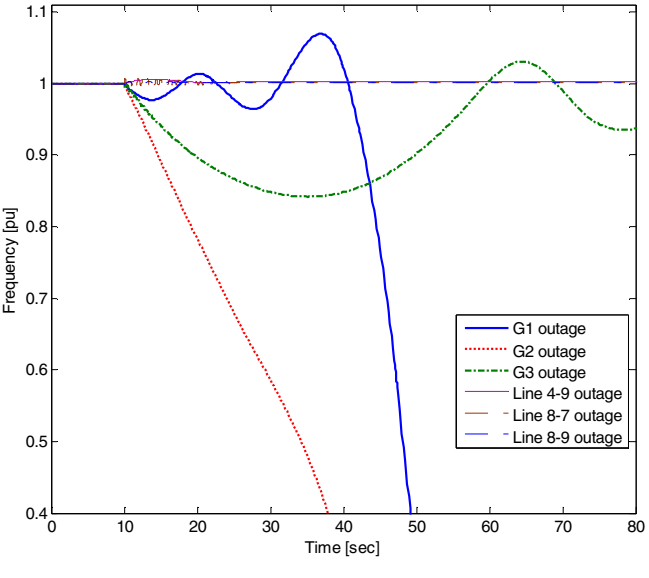

Fig. 8. Frequency deviation in different contingencies

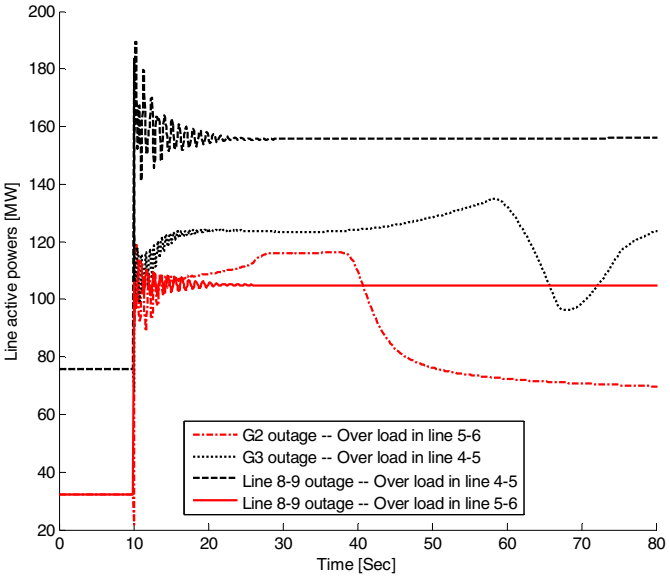

Fig. 9. Line over-loading in different contingencies

instability in an emergency condition. However, it is possible to see an inverse behavior during another test scenario. For example, considering Figs. 7 and 8 shows that diminishing of voltage is more considerable than frequency, when G1 is tripped.

Fig. 9 shows the system line powers, following a range of possible contingencies. This figure shows those line powers which are exceeded from the specified limits. It is shown that the outage of line 8-9 increases the overload on lines 4-5 and 5-6, significantly. This event may lead to lose these lines and to start a cascading failure.

In summary, the performed nonlinear simulations clearly indicate that individual monitoring of voltage and frequency may not determine the rate of severity for a contingency at the starting time of an event, securely. Both performance indices are needed to measure the severity rate of a contingency (see also G3 outage scenario in Figs. 7 and 8). It will be shown later that how the mentioned indices could be used for the sake of contingencies ranking.

4 Developed ANN-Based Emergency Control Scheme: An Overall View

4.1 Proposed Intelligent Control Framework

In the present chapter, a new intelligent emergency control is proposed. The developed emergency control scheme is summarized in Fig. 10. Following an event,

the first artificial neural network (ANN-1) labels the contingency by a specific number. If the predicted contingency is a sever one, it triggers the designed load shedding algorithm which is described in Section 1.5. For this purpose, an other trained neural network (ANN-2) uses the specified contingency number together with the measured tie-line active/reactive powers to estimate the system P-V curve. The amount of load should be shed is immediately computed using an estimated P-V curve. The main steps of the proposed algorithm are as follows:

1. At the first step, all contingencies should be identified and a special binary number to be allotted to each contingency. The sever contingencies have different binary numbers but for other contingencies an identical number is used. A special number is also considered for normal operation of the system. The contingency numbering process is done by the ANN-1.
2. The ANN-1 should be properly trained using the tie-lines active and reactive powers. The training data could be generated through a static analysis, and are used for a wide range of load patterns and various generation dispatching schemes. These scenarios are repeated for different contingencies.
3. The ANN-2 should be trained to predict the P-V curve. The inputs of ANN-2 are the severe contingency's number estimated in the previous step, and the tie-line active and reactive powers before the related event. The ANN-2 outputs are the coefficients of a 4^{th} degree polynomial function that estimate the P-V curve. It should be mentioned that ANN-2 is designed to predict the P-V curve for severe contingencies, only. Therefore, generation of training data is not so time consuming. The training data are generated for the various load patterns, generation dispatching scenarios, and the wind speeds. Finally the P-V curve is extracted and fitted by a 4^{th} degree polynomial function, which is described in Section 1.4.4. The updated weights after training of ANNs are saved, and then will be used to implement ANN-2 for the online prediction.
4. The estimated PV curve in the previous step is used to determine the amount of load that should be shed to move the operating point into a desirable region. The distance between operating point and the bounds of desirable region determines the cumulative amount of load which is needed in load shedding. The operating point on the PV curve is calculated by crossing the normal power (overall power system load before the contingency event e.g., 315 MW for the present test system) with PV curve. The desirable point is a point that the weakest bus voltage is upper than the allowable magnitude or the stability margin to be larger than the specified value (see Section 1.5.4).
5. A new load shedding algorithm (Section 5) is implemented to shed amount of load in the assigned steps based on simultaneous using of voltage and frequency indices. The cumulative amount of loads that should be shed is limited by the determined value in the previous step. When the cumulative amount of load shedding reaches to this limit the load shedding is interrupted for 10 seconds. After this relatively long delay, if more load shedding is needed, the load shedding will be continued. This delay also exists in the Florida Reliability Coordinating Council (FRCC) regional UFLS implementation schedule [37]. But it is noteworthy that, in the FRCC schedule, the 10 seconds delay is

used when the cumulative loads reaches to a predetermined value (about 41 percent of total the load).

6. To assign the first step of load shedding, the initial rate of frequency change is used to determine the amount of load that should be shed. For example if the magnitude of frequency gradient is larger than 1.5 Hz/sec, the amount of load that should be shed in the first step to be fixed at 15% (instead of 9%) of total power system load.

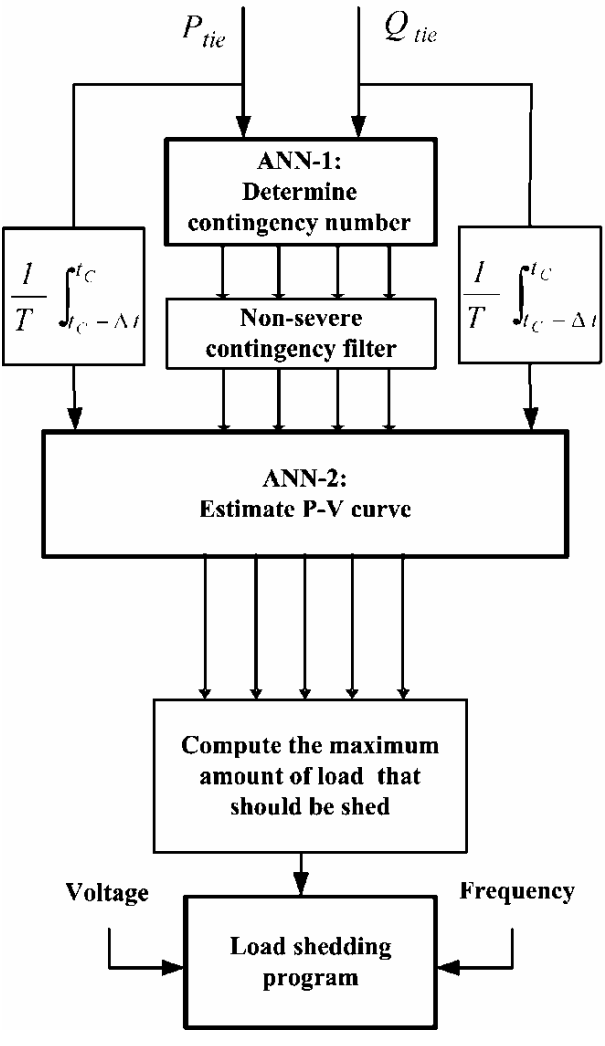

Fig. 10. The proposed intelligent power system emergency control scheme

4.2 Voltage Stability Margin and P-V Curve

In the proposed power system emergency control plan, the on-line predicting of P-V curves is used to determine the system stability margin. A P-V curve is generally obtained from the static studies, and for application in dynamic/real-time studies, it should be revised. On the other hand, a large penetration of wind turbines certainly affects the system P-V curves, which may not be clearly observed in a well-known pure static analysis.

Voltage Stability and Conventional Power Flow

Voltage stability is the ability of a power system to maintain/restore the voltages of all buses in a stable region after a disturbance [37]. The P-V curve is a suitable tool to estimate the stability margin of a power system around its operating point in the steady state. By increasing the load power connected to a bus, the bus voltage decreases and leads to change the voltages of other buses. Therefore, the system operating point moves, until reaches a point that no more power injection is possible. This is the bifurcation point and usually is used to determine the maximum load-ability of a system [20].

The behavior of the active power injection and bus voltage for two bus system can be calculated from the following equation [37].

$$V^4 + (2P.tan\emptyset - 1)V^2 + P^2.sec^2\emptyset = 0 \tag{3}$$

where V, P and $\emptyset$ are load bus voltage, active power absorbed by the load, and the angle between the active and reactive parts of load, respectively.

The critical point of this equation which shows the maximum load ability of the power system can be easily computed. For a power system with more than two buses, deriving a relationship between the active power injection and the bus bar voltages, and also tracing the P-V curve is not as simple as derived in (3). The reason is in complexity of the nonlinear power system equations that should be solved by appropriate recursive methods. Therefore, a power flow program should be run to achieve each point of P-V curve. By increasing the load power and near to the bifurcation point because of singularity of the Jacobin matrix in these points, the power flow equations cannot be solved.

To overcome above problem, the continuation power flow (CPF) method can be used via an appropriate predictor-corrector technique [36, 37]. Adding rows and columns to the Jacobin matrix, and predicting initial conditions for each point of P-V curve are helpful to solve the equations. In Fig. 11, the P-V curves of the IEEE 9-bus test system produced by the CPF method are shown. As illustrated, the maximum loadability of the given system is approximately limited to 720 MW.

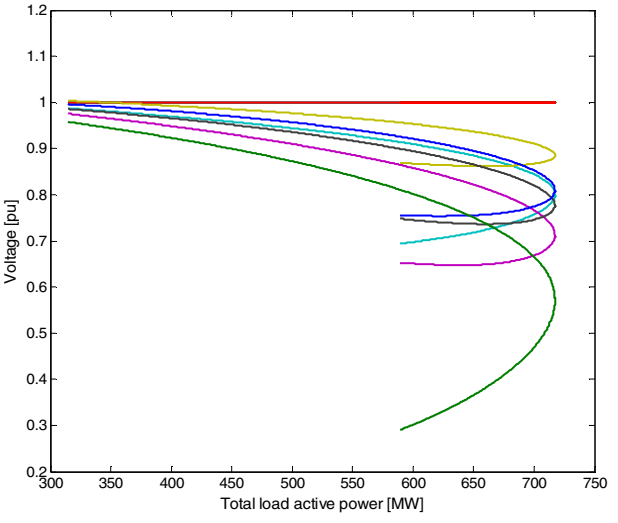

Fig. 11. The produced P-V curves by the static conventional CPF for the test system

With considering various important issues such as the generator Q-limits [26, 24], different bus load patterns and generator dispatching [31], the CPF method to be more useful. The same technique can be also used to analysis the line outages [15].

P-V Curves for Sudden Load Changes and Line/Generator Outage

As mentioned, the CPF method is known as a powerful tool for static voltage stability analysis. In this method, it is assumed that the rate of load change is slow, and all points on the P-V curve are in their steady state values. It is also assumed that all generators in the system have enough time to trace the load changes on the produced P-V curve. Since, the load variations are time dependent and the ability of power system to trace the load variations depends on the turbine governor droop characteristic, total power system reserve, the generator Q-limits, and the generator ramp rates. In other hand, an emergency condition following a sudden load change, generator trip or line outage is generally occurred in a short time. Therefore, using of P-V curve in the CPF techniques for an emergency control issue needs a revision [36].

Dynamic continuation power flow (DCPF) can be considered as a solution to plot the P-V curve in an emergency condition. In the DCPF, each point of a P-V curve is also known as a system equilibrium point. While, in emergency control strategies, such as the presented one in this chapter, the real-time voltage magnitude (not equilibrium point) is used to determine the voltage stability margin. To

achieve a more suitable P-V curve for the emergency control studies, it is needed to incorporate the load variation time in the P-V curve producing algorithm.

In the conventional CPF, a continuation parameter is defined to lead the operating point in the P-V curve tracing. This parameter can be moved between the state variables. Therefore, it is possible for the P-V trajectory to turn back after reaching to the bifurcation point. However, to implement the CPF in a time domain simulation, it is needed to use one continuation parameter only, that varies through tracing path, before and after the bifurcation point. To find a suitable parameter, consider the bellow equations [20, 36]:

$$S_L = P_L + jQ_L = V_L \times I_L{}^* = \frac{|V_L|^2}{Z_L{}^*} = Y_L{}^* \times |V_L|^2 \tag{4}$$

$$V_L = \frac{Z_L}{Z_L + Z_t} \times E_t \tag{5}$$

where S_L, Y_L, V_L, Z_L, Z_t, and E_t are load power, load admittance, equivalent load voltage, load impedance, transmission line impedance and bus voltage, respectively. Usually, the increasing of load power is the conclusion of adding more consumer devices to the power system. The loads as parallel admittances and adding more loads at a bus increase the equivalent admittance of the loads at the same bus. The voltage of the load bus V_L is decreased by increasing the load admittance Y_L (5). As it is shown in (4), Y_L and V_L determine the total power injection. At the beginning of an overload event, the increasing of Y_L is more considerable than decreasing of V_L; and in result the amount of power injection to be increased. But by adding more loads, the P-V curve reaches a point that the reduction of voltage square overcomes the increasing of the equivalent admittance and the power injection start to decrease. Based on above description the load admittance increases on the whole P-V curve trajectory. Therefore, it could be a suitable continuation parameter for the implementation of CPF in the time domain simulation. Using the Z-constant load model [20] and decreasing the load impedance during the simulation time with a proper rate, and measuring the load active power and its voltage, a full trajectory for the P-V curve will be produced. It should be noted that to solve the system differential equations, the simulator/solver software must be equipped with appropriate variable stepped-size techniques.

In comparison of conventional P-V curve producing methods, the above mentioned methodology in the time domain simulation environment contains following advantages:

1. By changing the rate of load admittance variation in the P-V curve tracing scenario, different P-V curves for different tasks such as short term and long term studies could be produced.
2. Many constraints, such as generator Q-limits, ramp-rates, droop-characteristics, and other limits could be easily included.
3. Various load patterns and generation dispatching scenarios could be considered.

4. Using the proposed method, it is possible to obtain the system P-V curves for sudden load changes in an emergency condition, while they cannot be achieved by the conventional CPF algorithms. It will be easily done by modeling the sudden load changes with a sleep slop ramp function.
5. The proposed method can be used to derive a P-V curve for the power system with WTGs by considering their dynamic models. It may be useful to explore unknown behaviors of the power system in the presence of wind turbines, and analyze their effects on the voltage stability margin [36].

It should be mentioned that using this analysis technique may not suitable for the fast dynamic cases such as fast contingency ranking. In the present emergency control scheme, this algorithm is only used for the severe contingencies. Fig. 12 compares the P-V curves derived by conventional CPF and above mentioned algorithm. As shown, the stability margin of a power system following a sudden load change is considerably less than one achieved by the steady state analysis. Therefore, to use the P-V curves in the emergency control strategies, a revision (like as explained above) is needed.

A comparison between the derived P-V curves using two different load rate changes is given in Fig. 13. The applied load variation patterns by increasing the load admittance are shown in Fig. 14. It can be seen that the stability margin for the rapid load change is less than the slow load change. These figures also show that the present method is capable to drive P-V curve for the rapid load change cases.

The P-V curves for the cases that a line or a generator is out of service or has been tripped are also important. When the system reaches its stable state, the tracing P-V curve scenario will be start. In order to plot P-V curve for the severe contingencies that

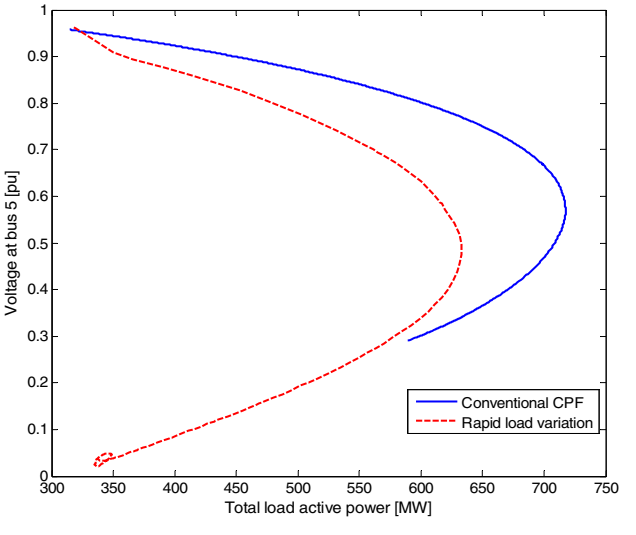

Fig. 12. P-V curves for the conventional CPF, and rapid load variation

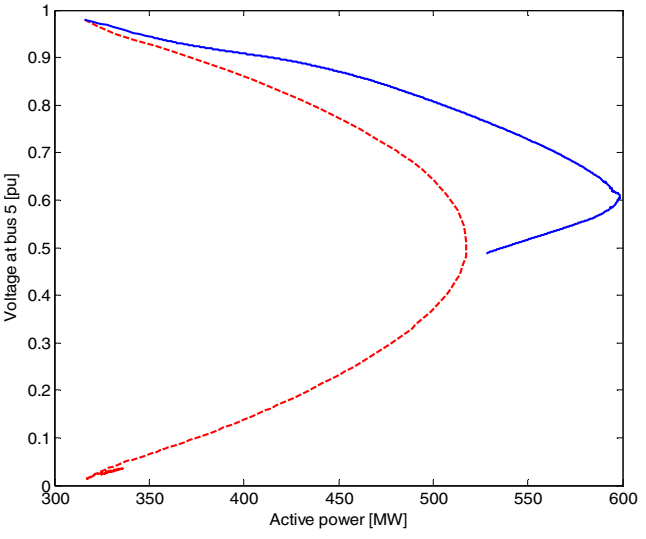

Fig. 13. P-V curve for the rapid (dashed) and slow (solid) load variation patterns (shown in Fig. 14). Only load at bus 5 has been changed

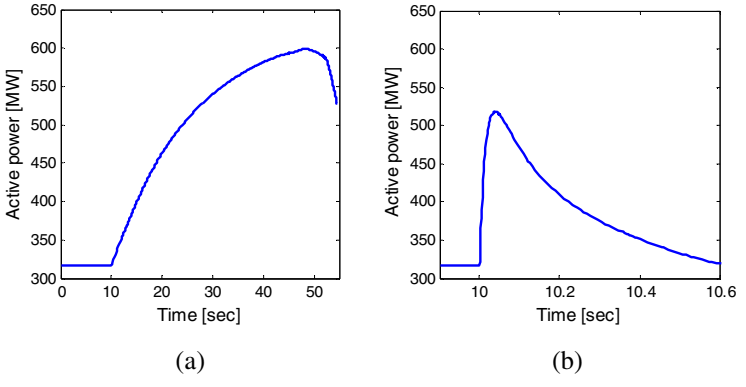

Fig. 14. Applied load variation patterns; (a) slow change, (b) rapid change

system never finds a stable state, an auxiliary technique should be used to lead the system into a stable condition. For example, one may curtails some load blocks to find a steady state instead of increasing the generator outputs.

The P-V curves for the normal (base case) condition and two different scenarios (line 8-9 and G1 outages) are shown in Fig. 15. These curves are achieved by immediate increasing load at bus 5. It is shown that the G1 outage is more unsecure than other test scenarios. The system stability margin is significantly reduced, when G1 is tripped.

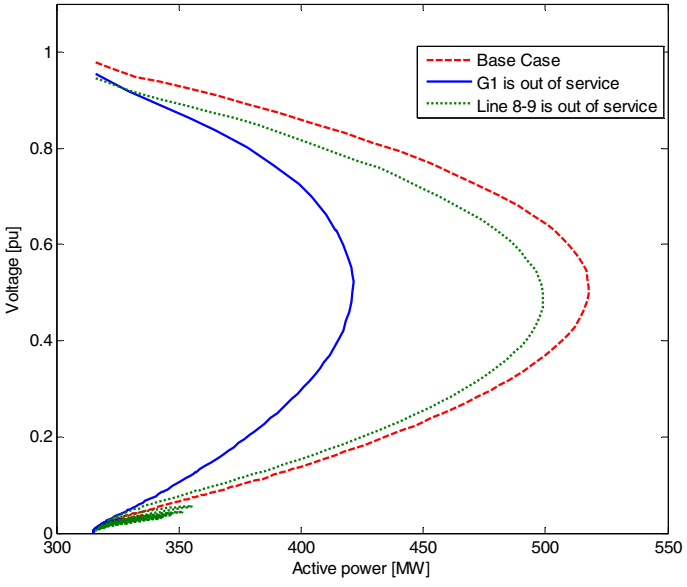

Fig. 15. P-V curves for two severe contingencies at the weakest bus

4.3 ANN-1 to Determine Contingency Number

In an emergency condition, an appropriate control decision should be immediately made. Therefore, using recursive algorithms to find optimal solutions are not implementable for this kind of situations. On the other hand, direct using of some tools such as deriving P-V curve to approach optimal solutions are usually time-consuming. However, these tools could be applicable, if one uses the fast estimation/prediction techniques. Because of predictability and immediate responsibility, the ANN can be considered as a powerful alternative to do the mentioned task.

A contingency number is an arbitrary code that determine which generator/line has been tripped. In order to obtain the contingency numbers, one may use remote terminal unit (RTU) signals in a supervisory control and data acquisition (SCADA) center. This method is too slow to use in an emergency condition. That is why, the measurements form the existing fast devises such as phase measurement units (PMU) are used to feed the performed neural network to provide a contingency number which actually shows the fault location.

Using P and Q by an ANN to predict the contingency number is suggested in this section. As shown in Fig. 10, if a severe contingency occurs in one of power system regions, the assigned ANN (ANN-1) is able to predict the contingency number by measuring the tie-line powers. This method could be also replaced by the existing methods that use the system frequency gradient as an input variable.

Selection of Input Variable

Selecting the features that used as input variables for the ANN-2 plays an important role in the efficiency of the proposed intelligent framework. The ANN-2 should be enough fast to response in a few milliseconds following a contingency event. Since, the majority of the variables oscillate in the contingency duration, using the measured values in a real-time measurement and making appropriate decisions based on results is difficult.

An experimental study (under specific assumptions) on the tie-line active powers measurement following loss of generation shows some interesting results. Fig. 16 shows the tie-line active powers following loss of G1.

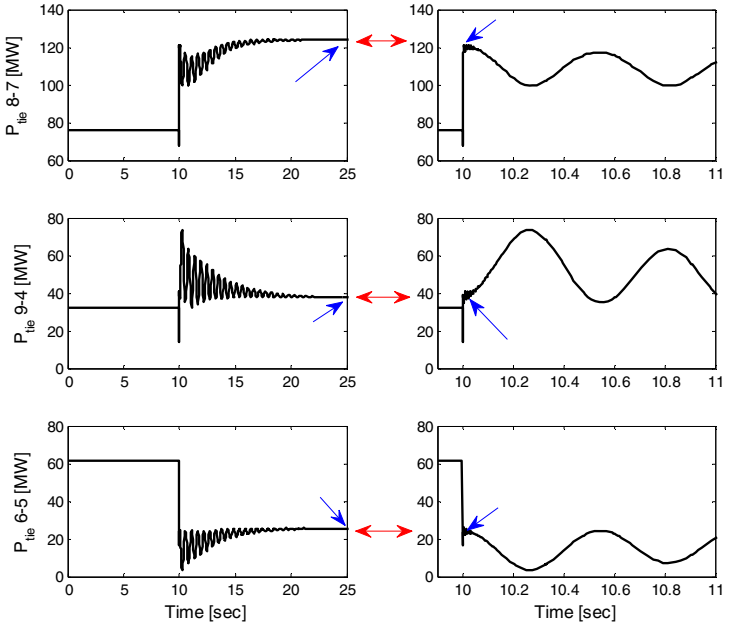

Fig. 16. Tie-line active powers following G1 loss; right-side figures show the zoomed views around 10s

As illustrated, the values of line active powers during a few milliseconds after the contingency (right-side column in the figure) are equal to their steady state values that could be derived even from the steady state power flow programs. Fig. 17 shows this phenomenon in the presence of DFIG type WTGs. In the emergency control strategies it is important to find a picture from the post contingency conditions, and analyze it to make a suitable decision and effective control action. Based on the above study the tie-line powers are used as inputs for ANN-1 to determine the contingency at the beginning of a serious fault.

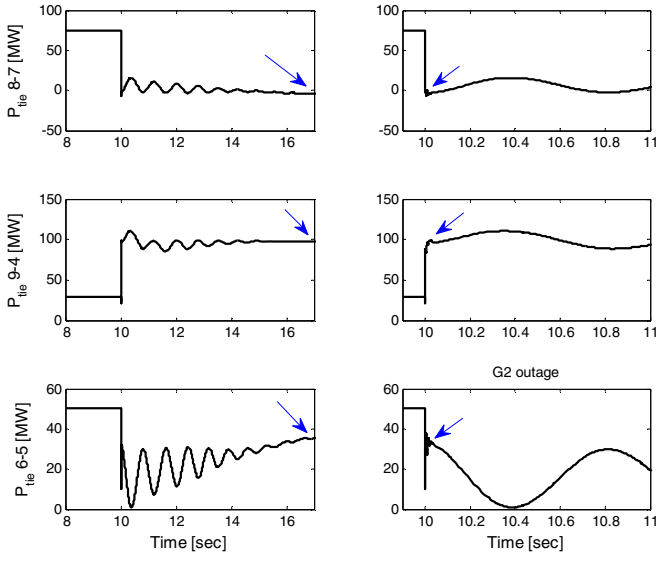

Fig. 17. Tie-line active powers in the presence of DFIG following G2 loss; right-side figures show the zoomed views around 10s

Identify the Contingency Number

As shown in Fig. 15, the P-V curves completely depends on the power system topology. The line/generator outage affects the P-V curves, significantly. In the other hand, the performance of an ANN is considerably depended on the features that used as ANN inputs [30]. The main target of ANN-2 is to estimate the power system P-V curve following a serious event to determine the maximum amount of load for shedding, in order to restore the power system operating point into a point with an acceptable stability margin.

The performed study shows that using the tie-line active and reactive powers as inputs are not adequate to predict the P-V curve. Extracting suitable new features and adding them to the inputs array make ANN-2 more efficient. The new features must concern the power system topology.

The inputs of the first ANN (ANN-1) are the tie-lines active and reactive powers and the output is a binary code representing the number of a severe contingency. For each severe contingency, a specific number is allotted and for all other (non-severe) ones an identical number is allotted. Fig. 18 shows the outputs of ANN-1 following loss of G3. The number that allotted for this contingency is 3, and the number that allotted to the base (normal) case is 7. As shown, the output of the power system before the contingency is 0111 and after loss of G3 is 0011. It should be mentioned that appropriate thresholds are applied to the outputs of the ANN-1, such that the binary digits bellow 0.5 are considered as 0, and above 0.5 are fixed at 1.

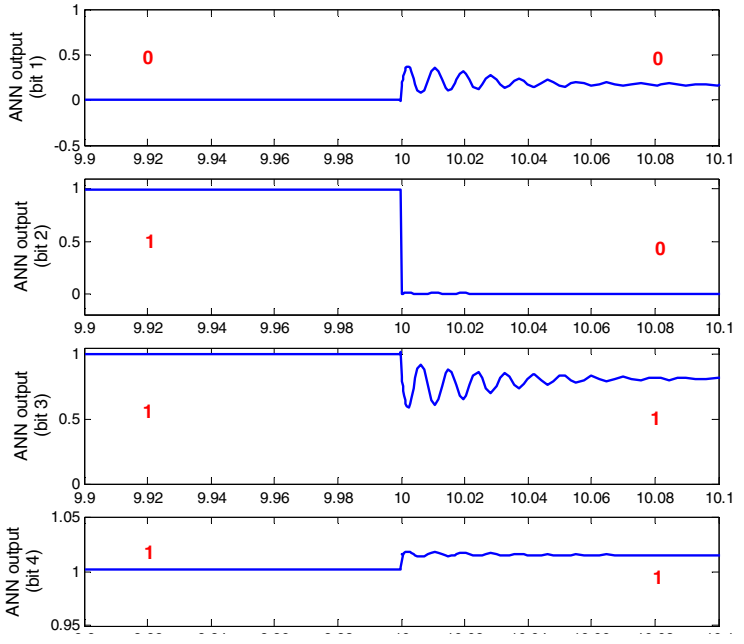

Fig. 18. The output of ANN exactly at the time of G3 outage. The target output for this case is the binary digits 0011 (3).

4 ANN-2 to Estimate the P-V Curve

The ANN-2 target is estimating of system P-V curve for post-contingency topology in a few milliseconds following a serious event. The method used for this purpose should satisfy some characteristics. It must be enough fast, and should consider system topology and various uncertainties due to variable nature of load, generation and wind speed.

The Thevenin's equivalent circuit for an existing real power system is known as a solution to formulate power system topology [33]. However, on-line finding of an appropriate Thevenin's equivalent system concerning the variable nature of load, complexity of real system, various uncertainties and practical constraints, specifically in the presence of wind turbines is difficult.

Considering the real-time prediction property and learning ability of neural networks, the ANN-2 is designed to solve above problem. In order to taken account the system post fault topology, the contingency information is used as the ANN-2 input.

As has already mentioned, the contingencies are numbered and the numbers can be identified in a few milliseconds after the contingency event by ANN-1, or

an alternative method. For the example at hand, contingencies are numbered as four digits binary codes.

Furthermore, the tie-line active and reactive powers are used to formulate the load/generation and wind speed changes. As shown in Fig. 10, the average of these powers among Δt (here, 5 seconds) before the contingency is supplied to the ANN-2. This input can be formulated as follows.

$$P_{ave} = \frac{1}{T}\int_{t_C-5}^{t_C} P(t)dt \ , \ Q_{ave} = \frac{1}{T}\int_{t_C-5}^{t_C} Q(t)dt \tag{6}$$

where, t_C is the time of fault (contingency time), P (Q) is the tie-line active (reactive) power, and T is the time period (here, $T = \Delta t = 5s$).

The output layer of ANN-2 includes five neurons, corresponding to the coefficients of a four-degree polynomial function to estimate the P-V curve in the following form,

$$P = a_1V^4 + a_2V^3 + a_3V^2 + a_4V^1 + a_5 \tag{7}$$

where a_1 to a_5 to be determined by the outputs of ANN-2. The data for above P-V curves is produced by the algorithm described in Section 1.4.2. The developed P-V curve estimation method is applied to the test system.

A comparison between original and estimated P-V curves (using the given 4th order polynomial in (7)) for three tests (normal operation, G2 outage, and line 8-9 outage) are shown in Fig. 19. The obtained polynomial coefficients (7) are given in Table 1.

Table 1. 4th order polynomial coefficients

		a_1	a_2	a_3	a_4	a_5
Case1:	Target	0.9349	-2.7315	-0.3821	2.0858	0.0118
Normal operation	Predicted	0.9237	-2.6442	-0.4827	2.1199	0.0088
Case2:	Target	0.2960	-1.4384	0.0129	1.0492	0.0048
G1 outage	Predicted	0.2347	-1.2797	-0.1056	1.0721	0.0021
Case3:	Target	-0.3862	0.3249	-2.7286	2.7086	-0.0694
Line 8-9 outage	Predicted	-0.5644	0.6790	-2.9786	2.7757	-0.0759

4.5 ANN-1 and ANN-2 Configurations

A three layer back-propagation neural network is used for both ANN-1 and ANN-2. The activation functions for the hidden layers are in form of tangent-sigmoid function, and the output activation functions are linear.

The number of neurons in hidden layer is chosen via try and error method, and for the scaling of neural network's inputs/outputs, *min-max* method is applied. The parameters of applied min-max function to the training data are saved and will be used for the actual test data. Fig. 20 shows a general configuration of ANN-1 and ANN-2 for the online applications.

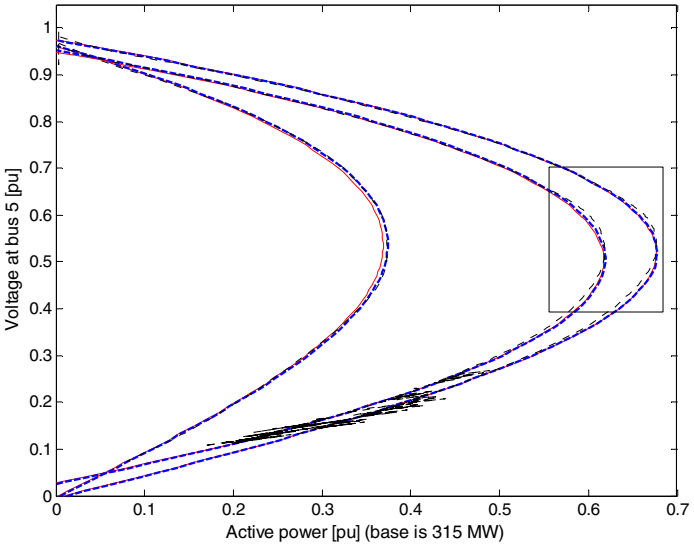

(a)

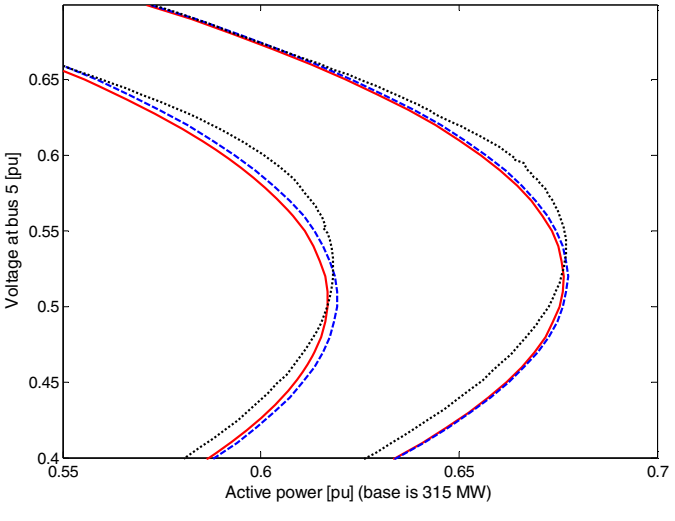

(b)

Fig. 19. P-V curves; ANN-2 output (solid), Original (dotted), and fitting by polynomial (dashed). Figure (b) shows a zoomed view around 0.6 pu.

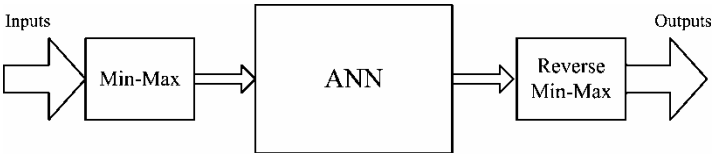

Fig. 20. ANN configuration for the online application; the min-max and reverse min-max parameters come from training data

In the min-max method, each element of the input/output vector is mapped into interval [-1, 1], based on the training data samples corresponding to the following variable.

$$y_i^t = (y_{max} - y_{min}) \frac{x_i^t - x_{min}^i}{x_{max}^i - x_{min}^i} + y_{min} \tag{8}$$

where, x_i^t is the *i*-th element of the *t*-th sample vector of the training data, y_i^t is the *i*-th element of the *t*-th sample vector of the training data mapped into the interval [-1, 1], and $x_{max}^i(x_{min}^i)$ is the maximum (minimum) value of the training vector that contains *i*-th input/output element (here, $y_{min} = -1$, and $y_{max} = 1$).

Therefore, for each input and output vector elements there are a minimum and a maximum values derived from training data. These values should be saved and used beside the trained neural network for predicting purposes.

The used tangent sigmoid activation function is as follows:

$$f(x) = \frac{2}{1 - e^{-x}} - 1 \tag{9}$$

For learning of neural network, the corresponding P-V curves for both normal operation and major contingencies (which are identified in the contingency ranking step) should be obtained. The proposed ANN-2 has 10 linear neurons in its first layer, corresponding to the number elements in the input vector (3 tie-line active powers, 3 tie-line reactive powers, and 4 digits for the contingency number). The number of neurons in form of sigmoid function (8) is 15, and the number of output neurons is fixed at 5; corresponding to the coefficients of estimating polynomial (7).

5 A New Load Shedding Algorithm

5.1 Load Shedding

Load shedding (LS) is one of emergency control actions to protect the system following a major fault which seriously deviates the system frequency and/or voltage. The LS curtails amount of load in the power system until the available generation could supply the remind loads. If the power system is unable to supply its active and reactive load demands, the under-frequency and under-voltage conditions will be intense. Many algorithms for UFLS and UVLS have been proposed

[2, 3, 6, 13, 15, 28, 35, 29]. The number of LS steps, amount of load that should be shed in each step, the delay between the stages, and the location of shed load are the important objects that should be determined in an LS algorithm.

To prevent the post-load shedding problems and over loading, the location bus for LS will be determined based on the load importance, cost, and distance to the contingency location. The most LS schemas proposed so far used voltage and frequency parameters, separately. The underfrequency and undervoltage relays are working in the power system without any coordination. Following, some examples are given to illustrate the necessity of considering both of voltage and frequency indices to achieve a more effective/adaptive and comprehensive LS scheme.

5.2 Simultaneous Using of Voltage and Frequency

In this section, it is shown that considering both voltage and frequency indices are needed to achieve a more effective emergency control plan [36]. Fig. 21 shows the voltage and frequency deviations for two different LS scenarios following the same contingency. In these tests, G1 is tripped at 10s. In scenario 1, only 9% of total system active power is curtailed, while in scenario 2, in addition to 9% active power, 9% of total reactive power is also discarded. Both scenarios shed the load when the frequency falls below 59.7 Hz as used in some existing LS standard such as FRCC standard [14]. Considering the frequency and voltage behavior in the performed two scenarios, some important points are achieved.

A majority of published research on the UFLS issue considered the active part of load only; while by considering the reactive power part, the frequency decline will be affected as shown in Fig. 21b. Furthermore, in the actual power system, the loads contain both active and reactive parts. Figs. 21a and 21b do not show which scenario is more effective. Fig. 21a illustrates a better performance for scenario 2, while Fig. 21b shows an inverse result. This simulations show that by individual monitoring/using of frequency and voltage there is no guaranty to achieve an effective LS strategy.

Recall Figs. 2, 4 and, 5 and consider the frequency and voltage deviation for the case that IG with STATCOM is interconnected to the power system. Fig. 2b shows that the post contingency voltage behavior of the system in the case of IG with STATCOM is much better than IG without STATCOM, while Fig. 4 shows an inverse result for the system frequency response. Fig. 5 also shows that voltage and frequency may behave in the opposite directions.

From above descriptions and the performed simulation results, it is realized that considering just one of frequency and voltage indices cannot lead to an effective/optimal LS plan, especially when the reactive power is incorporated into studies. The WTGs generally use induction generators that consume the reactive power. The FACTS devices are usually used to compensate the reactive power for these cases may influence the amount of frequency decline.

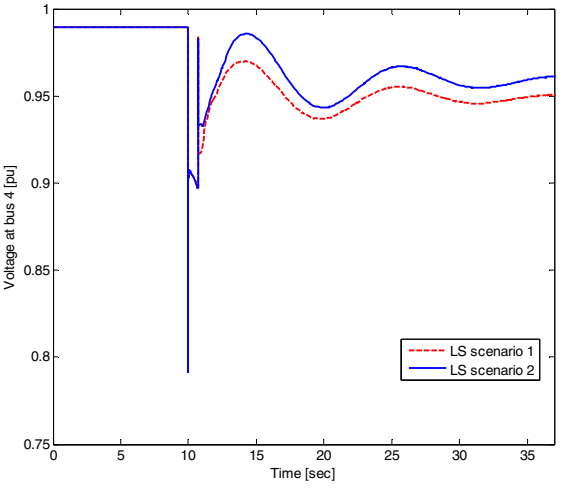

(a)

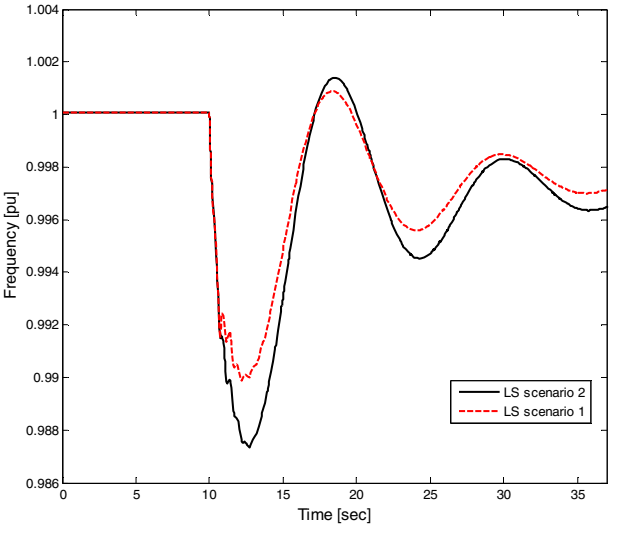

(b)

Fig. 21. System response for two different LS scenarios; a) voltage deviation, b) frequency deviation

5.3 Proposed LS Algorithm

The coordination between conventional UFLS and UVLS as separate algorithms is very difficult and even may be impossible. Therefore, both voltage and frequency should be used in the same LS program, simultaneously.

Following a contingency event, the power system operating point deviates from its stable pre-contingency state. If the contingency is not severe enough, the system may converge to another stable point. Otherwise, the system states move to unstable region. As mentioned, for the emergency control purposes, voltage and frequency are two suitable observable variables that could illustrate the state of system following an event. Fig. 22 shows the trajectory of the system states in the voltage-frequency plane, following a contingency with two scenarios: unstable trajectory, and stabilized trajectory using an LS plan. The states that used in this trajectory are Δf and ΔV, as follows.

$$S = \widehat{\Delta f} + j\widehat{\Delta V} \tag{10}$$

and,

$$\widehat{\Delta f} = \frac{\Delta f}{f_0}, \qquad \widehat{\Delta V} = \frac{\Delta V}{V_0} \tag{11}$$

where, f_0 and V_0 are the frequency and voltage before contingency. To design a new LS algorithm based on the above state variables, some threshold boundaries should be defined instead of threshold values that are used in the conventional LS algorithms.

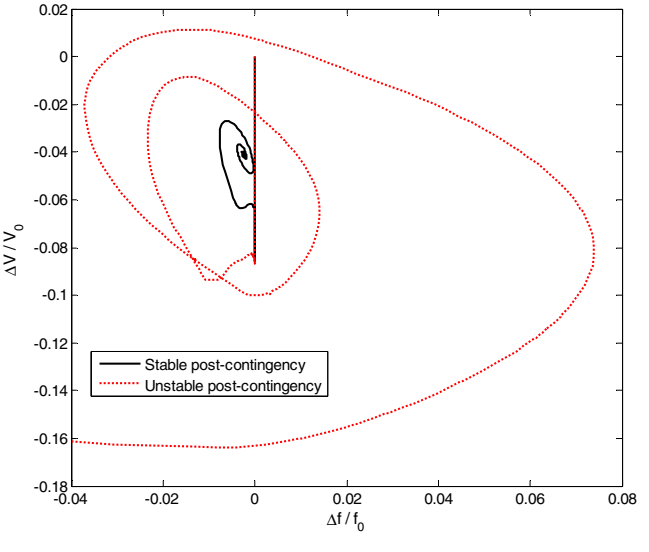

Fig. 22. Phase trajectory for stable and unstable post-contingency scenarios

One may suggest the circular boundaries. But since the threshold movement sizes in two directions (the UFLS and the UVLS) are not the same, the elliptical boundaries are much better. Therefore, assuming

$$x^t = \widehat{\Delta f} = \frac{f_t - f_0}{f_0}, \; y^t = \widehat{\Delta V} = \frac{V_t - V_0}{V_0} \tag{12}$$

and according to Fig. 23, the control load shedding (CLS) switches can be defined as follows:

$$CLS_i = \left(\frac{x^t}{a_i}\right)^2 + \left(\frac{y^t}{b_i}\right)^2 \tag{13}$$

Where, the x^t and y^t are new variable states. The f_t and V_t are the frequency and voltage at time *t*. The a_i and b_i parameters can be computed as shown in Table 2, and the threshold can be fixed in a point satisfying CLS_i>1. As shown in Table 2, the overall framework of the present LS scheme is close to the LS schedule introduced by FRCC [14], and it is rewritten in Appendix (Table 7).

Each step is determined by an ellipse and when the phase trajectory reaches to each ellipse, the corresponding LS step will be triggered. Fig. 23 shows the LS steps on the phase trajectory plan in the case of losing G2, the largest generator in the test system. The time delay between steps should be added to the LS algorithm. The voltage and frequency may need to pass through a low pass filter before entering into the algorithm. Existing practical constraints should be also, considered in the proposed scheme.

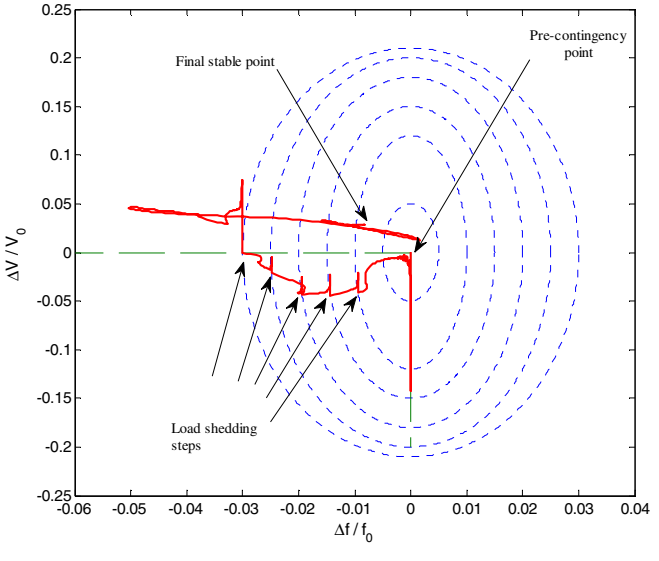

Fig. 23. New LS scheme

Table 2. New LS schedule

LS Steps	a_i	b_i	Time delay [sec]	LS (%)
A	0.3/60	0.05	0.28	9
B	0.6/60	0.12	0.28	7
C	0.9/60	0.15	0.28	7
D	1.2/60	0.18	0.28	6
E	1.5/60	0.2	0.28	5
F	1.8/60	0.21	0.28	7
….			….	

The initial conditions at time of each LS step are an important factor to obtain a more effective protection plan. For example, shedding the load in the conditions that voltages of the buses are above their pre-contingency values may result more bad circumstance.

That is why, in the proposed algorithm, the loads are allowed to be shed only at the third quarter of the phase trajectory plane. In order to prevent shedding of load in the voltage dip conditions (e.g., when a short circuit is not eliminated and the frequency is decreased while the voltage is normal), a specific margin will be considered. Based on this margin, the loads are allowed to shed only when the angle of S in (4) is between ($\pi+\alpha_1$) and ($\frac{3\pi}{2} - \alpha_2$).

The phase trajectory of the presented LS algorithm that contains time delay and dead-margin is shown in Fig. 24. Because of time delay, the LS steps are not exactly fired on the elliptical borders. Fig. 25 shows the system voltage response at bus 4, following loss of G2. The new LS scheme is compared with the conventional UFLS. It is shown that the new LS scheme is more efficient to prevent over load shedding and over voltage conditions after running the algorithm.

5.4 Determine Amount of Cumulative Load That Should Be Shed

The ANN-2 output determines the coefficients of the polynomial function (7) that estimate the P-V curve of the power system. In the present chapter, this curve is used to predict the amount of load that should be shed to stabilize the system after a severe contingency. Here, it is explained that how the P-V curve is applicable for the mentioned purpose.

The P-V curve is simply estimated using a polynomial function and the designed neural network. The horizontal axis of the P-V curve which is obtained from the ANN-2 output is in per-unit at the base of total power system load, and only the amount of load that is added to the power system is considered. As has mentioned, to produce a P-V curve following a severe contingency, it may be needed to curtail some loads manually to lead the power system operating point to a stable point before starting the scenario. By considering these points, the P-axis of the P-V curve to be re-scaled as follows.

$$P_{new} = P_{old} \times P_{base} - P_c + P_{base} \tag{14}$$

where, P_{old}, P_{base}, P_c and, P_{new} are per-unit values of P-axis, base case total active power, manually curtailed active load, and re-scaled P-axis, respectively.

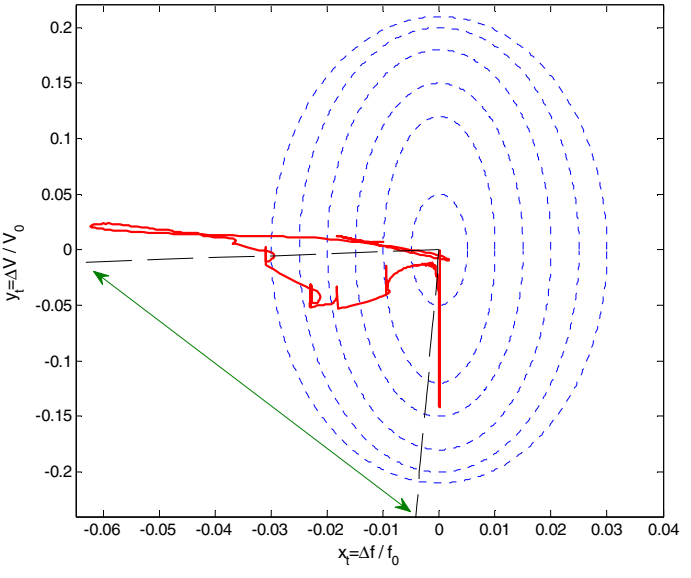

Fig. 24. The proposed LS scheme considering time delay and the permitted shedding region

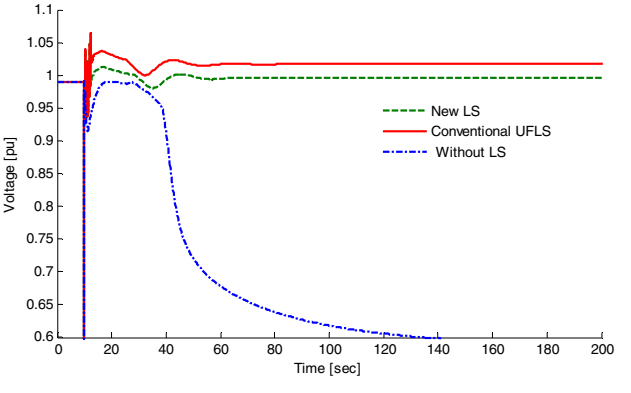

Fig. 25. Bus 4 voltage using different LS schemes following loss of G2

Using the produced P-V curve, the amount of load that should be shed could be calculated by means of one of following methods: 1) shed amount of load to re-store the power system bus voltages upper than a minimum permissive voltage

value (for example, 0.95 pu), 2) shed amount of load to achieve a minimum permissive power system voltage stability margin.

As shown in Fig. 26, the stability margin is defined as distance between the power system operating critical points. The critical point is the saddle node of the P-V curve, or it can be defined as a point that its corresponding voltage value reaches to a permissive value (for example, 0.8 pu [29]). Fig. 26 shows the P-V curve for the case of G2 outage. To provide this curve, 125 MW has been manually curtailed after making the G2 out of service. This curve is predicted by ANN-2, and re-scaled by means of equation (1.14). For the sake of comparison, the PV curve for the base case (normal operation) is also shown in Fig. 26. In the present example, the base case active load is 315 MW. By intercrossing the vertical line of 315 MW with the produced PV curve, the post-contingency power system operating point to be estimated. By considering this point and using one of above described methods, the amount of load that should be shed will be calculated. For example, as shown in Fig.26, to restore the bus voltages to 0.95 pu, it is needed to shed amount of 96 MW system load.

The LS steps and the amount of shaded load in each step are illustrated in Fig. 27. As shown in this figure, the cumulative load that should be shed is fixed to 96MW. Fig. 28 shows the system voltage and frequency deviation following application of the proposed emergency control strategy. In the performed simulations, all wind turbines are DFIG type, which supply ten percent of total system load.

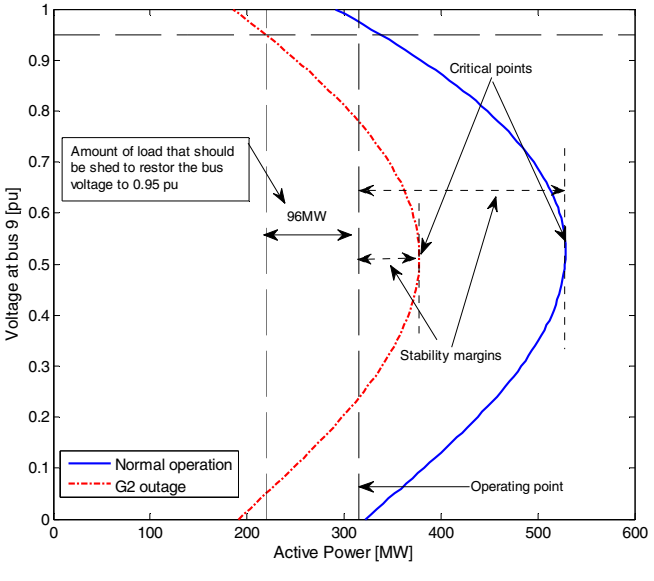

Fig. 26. Determine amount of load that should be shed after loss of G2

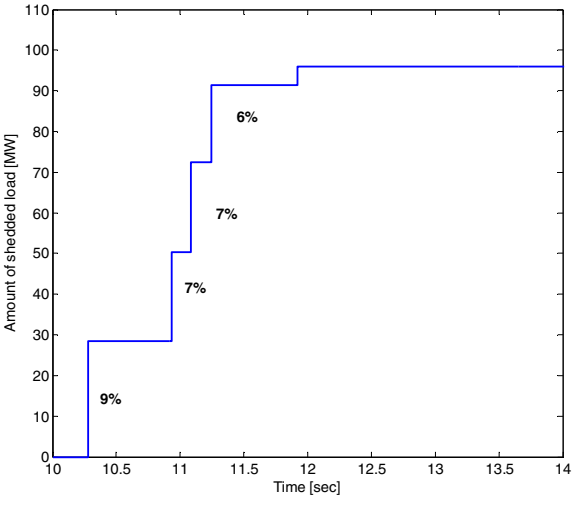

Fig. 27. The LS steps and amount of load that should be shed in each step in the case of G2 outage

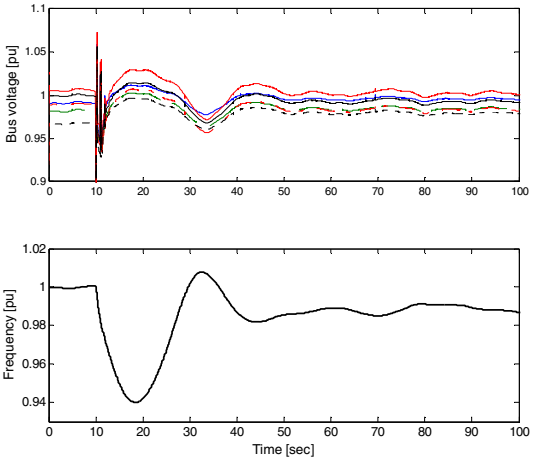

Fig. 28. System voltage and frequency deviation, following loss of G2

6 Summary

This chapter presents a new intelligent based power system emergency control scheme in the presence of high wind power penetration. The impacts of wind power fluctuation on the system frequency, voltage and frequency gradient are

analyzed, and an overview of the key issues in the use of wind power penetration in power system emergency control is addressed.

The necessity of considering both system frequency and voltage indices to design an effective load shedding algorithm is shown. Then, an intelligent artificial neural network (ANN) based emergency control scheme considering the dynamic impacts of wind turbines is proposed.

The ANNs are effectively used to identify severe contingencies and to estimate the system security level by predicting the post-fault stability margin. An ANN based methodology to estimate the post-contingency power-voltage (P-V) curve is introduced, and finally, the results are used to run an optimal load shedding algorithm. The proposed emergency control scheme and discussions are supplemented by computer nonlinear simulations on the IEEE 9-bus test system.

References

1. Alexander, J.F., Renuka, G., Jayabharath, R.D.: New Power Sensitivity Method of Ranking Branch Outage Contingencies for Voltage Collapse. IEEE Transactions on Power Systems 17(2), 265–270 (2002)
2. Bevrani, H.: Robust Power System Frequency Control. Springer, New York (2009)
3. Bevrani, H., Ledwich, G., Ford, J.J.: On the Use of df/dt in Power System Emergency Control. In: Proceedings 2009 IEEE Power Systems Conference & Exposition, Seattle, Washington, USA (2009)
4. Bevrani, H., Ledwich, G., Dong, Z.Y., Ford, J.J.: Regional Frequency Response Analysis under Normal and Emergency Conditions. Electric Power Systems Research 79, 837–845 (2009)
5. Bevrani, H., Ledwich, G., Ford, J.J., Dong, Z.Y.: On Power System Frequency Control in Emergency Conditions. Journal of Electrical Engineering & Technology 3(4), 499–508 (2008)
6. Bevrani, H., Hiyama, T.: On Load-Frequency Regulation with Time Delays: Design and Real Time Implementation. IEEE Transactions on Energy Conversion 24(1), 292–300 (2009)
7. Bevrani, H., Ghosh, A., Ledwich, G.: Renewable Energy Resources and Frequency regulation: Survey and New Perspectives. Will be submitted to IET Renewable Power Generation (2009)
8. Bijwe, P.R., Nanda, J., Puttabuddhi, K.L.: Ranking of line outages in an AC-DC system causing overload and voltage problems. IEE Proceedings-C 138(3), 207–211 (1991)
9. Claudio, A.C., Nadarajah, M., Federico, M., John, R.: Linear Performance Indices to Predict Oscillatory Stability Problems in Power Systems. IEEE Transactions on Power Systems 19(2), 1104–1114 (2004)
10. Ejebe, G.C., Wollenberg, B.F.: Automatic Contingency Selection. IEEE Transactions on Power Apparatus and Systems PAS-98(1), 97–109 (1979)
11. El-Saadawi, M.M., Kaddah, S.S., Osman, M.G., Abdel-Wahab, M.N.: Impact of wind farms on contingent power system voltage stability. In: 12th International Middle-East Power System Conference, pp. 637–644 (2008)

12. Erlich, I., Rensch, K., Shewarega, F.: Impact of large wind power generation on frequency stability. In: Proc. of Power Engineering Society General Meeting (2006) (CD ROM)
13. Ford, J.J., Bevrani, H., Ledwich, G.: Adaptive Load Shedding and Regional Protection. International Journal of Electrical Power and Energy Systems 31, 611–618 (2009)
14. FRCC Automatic Underfrequency Load Shedding Program, PRC-006-FRCC-01 (2009), https://www.frcc.com/
15. Fu, X., Wang, X.: Load Shedding Scheme Ensuring Voltage Stability. In: Power Engineering Society General Meeting IEEE, pp. 1–6 (2007)
16. Gillian, L., Alan, M., Mark, O.M.: Frequency Control and Wind Turbine Technologies. IEEE Transactions on Power Systems 20(4), 1905–1913 (2005)
17. Gu, X., Canizares, C.A.: Fast prediction of load ability margins using neural networks to approximate security boundaries of power systems. IET Gener. Transm. Distrib., 466–475 (2007)
18. IEEE PES, power and energy magazine 7(2), March/April Issue (2009)
19. Jadid, S., Jalilzadeh, S.: Application of Neural Network for Contingency Ranking Based on Combination of Severity Indices. In: Proceedings of World Academy of Science, Engineering and Technology, vol. 5 (2005)
20. Kundur, P.: Power System Stability and Control. McGraw-Hill, New York (1994)
21. Marcus, V.A.N., Ja, P.L., Hans, H.Z., Ubiratan, H.B., Rogério, G.A.: Influence of the Variable-Speed Wind Generators in Transient Stability Margin of the Conventional Generators Integrated in Electrical Grids. IEEE Transactions on Energy Conversion 19(4), 692–701 (2004)
22. Moura, R.D., Prada, R.B.: Contingency screening and ranking method for voltage stability assessment. IEE Proc.-Gener. Transm. Distrib. 152(6), 891–898 (2005)
23. Mukhtiar, S., Ambrish, C.: Power Maximization and Voltage Sag/Swell Ride- through Capability of PMSG based Variable Speed Wind Energy Conversion System. In: Annual Conference of IEEE on Industrial Electronics, vol. 34, pp. 2206–2211 (2008)
24. Naoto, Y., Hua-Qiang, L., Hiroshi, S.: A Predictor/Corrector Scheme for Obtaining Q-Limit Points for Power Flow Studies. IEEE Transactions on Power Systems 20(1), 130–137 (2005)
25. Oscar, E.M.: A Spinning Reserve, Load Shedding, and Economic Dispatch Solution by Bender's Decomposition. IEEE Transactions on Power Systems 20(1), 384–388 (2005)
26. Pengcheng, Z., Gareth, T., Malcolm: A Novel Q-Limit Guided Continuation Power Flow Method. In: Power and Energy Society General Meeting - Conversion and Delivery of Electrical Energy, July 20-24, pp. 1–7 (2008)
27. Power Systems Relaying Committee, IEEE Guide for the Application of Protective Relays Used for Abnormal Frequency Load Shedding and Restoration. IEEE Std C37.117™, pp. c1–c43 (2007)
28. Faranda, R., Pievatolo, A., Tironi, E.: Load Shedding: A New Proposal. IEEE Transactions on Power Systems 22(4), 2086–2093 (2007)
29. Mark, S.H., Keith, A.H., Robert, A.J., Lee, Y.T.: Slope-Permissive Under-Voltage Load Shed Relay for Delayed Voltage Recovery Mitigation. IEEE Transactions on Power 23(3), 1211–1216 (2008)
30. Simon, H.: Neural Network a Comprehensive foundation. Prentice hall international, Inc., Englewood Cliffs (1999)
31. Shao-Hua, L., Hsiao-Dong, C.: Continuation Power Flow with Multiple Load Variation and Generation Re-Dispatch Patterns. In: Proc of Power Engineering Society General Meeting (2006) CD ROM

32. Smith, J.C.: Winds of change: Issues in utility wind integration. IEEE Power Energy Mag. 3(6), 20–25 (2005)
33. Shu-Jen, S.T., Kim-Hoi, W.: Adaptive Under-voltage Load Shedding Relay Design Using Thevenin Equivalent Estimation. In: Power and Energy Society General Meeting, pp. 1–8, July 20-24 (2008)
34. Tarlochan, S.S., Lan, C.: Contingency Screening for Steady-State Security Analysis By Using FFT and Artificial Neural Networks. WEE Transactions on Power Systems 15(1), 421–426 (2000)
35. Thelma, S.P.F., Lenzi, J.R., Miguel, A.M.: Load Shedding Strategies Using Optimal Load Flow with Relaxation of Restrictions. IEEE Transactions on Power Systems 23(2), 712–718 (2008)
36. Tikdari, A.: Load Shedding in the Presence of Renewable Energy Sources in a Restructured Power System Environment, Master Thesis, University of Kurdistan (2009)
37. Venkataramana, A.: Computational Techniques for Voltage Stability Assessment and Control. Springer, Heidelberg (2006)
38. Venkataramana, A., Colin, C.: The Continuation Power Flow a Tool for Steady State Voltage Stability Analysis. Transactions on Power Systems 7(1), 416–423 (1992)
39. Vladimir, V.T.: Under-frequency Load Shedding Based on the Magnitude of the Disturbance Estimation. IEEE Transactions on Power Systems 21(3), 1260–1266 (2006)
40. Vidya, S.S.V., Nutakki, D.R.: Contingency Screening through Optimizing Hopfield Neural Networks Canadian Conference on Electrical and Computer Engineering, vol. 1, pp. 199–204 (1993)
41. Yeu, R.H., Sauer, P.W.: Post-Contingency Equilibrium Analysis Techniques for Power Systems. In: Annual North American Power Symposium, vol. 37, pp. 429–433 (2005)
42. Yongning, C., Yanhua, L., Weisheng, W., Huizhu, D.: Voltage Stability Analysis of Wind Farm Integration into Transmission Network. In: International Conference on Power System Technology, pp. 1–7 (2006)
43. Yuri, V.M., Viktor, I.R., Vladimir, A.S., Nikolai, I.V.: Blackout Prevention in the United States, Europe, and Russia. IEEE Transactions on Energy Conversion 14(3), 749–753 (1999)

Appendix

- Nine-bus test system simulation data

Table 3. Branch data

From bus	To bus	R (pu)	X (pu)	B (pu)	Limit (MW)
1	4	0	0.0576	0	200
4	5	0.017	0.092	0.158	200
5	6	0.039	0.17	0.358	100
3	6	0	0.0586	0	250
6	7	0.0119	0.1008	0.209	100
7	8	0.0085	0.072	0.149	200
8	2	0	0.0625	0	200
8	9	0.032	0.161	0.306	200
9	4	0.01	0.085	0.176	200

Table 4. Generator data

Generator	G1	G2	G3
Nominal Power [MVA]	128	247.5	192
Type	Hydro	Steam	Steam
Speed [rpm]	180	3600	3600
$V_{L\text{-}L}$ [KV]	16.5	18.3	13.8
X_d	0.146	0.8958	1.3125
X'_d	0.0608	0.1198	0.1813
X''_d	0.205	0.155	0.22
X_q	0.0969	0.8645	1.2578
X'_q	0.0969	0.1969	0.25
X''_q	0.221	0.143	0.292
X_L	0.0336	0.0521	0.0742
T'_d	8.96	6	5.89
T''_d	0.02	0.02	0.02
T'_{qo}	0.00002	0.535	0.6
T''_{q0}	0.02	0.02	0.02
R_S	2.8544e-3	2.8544e-3	2.8544e-3
H (on 100MW)	23.64	3.01	6.4

Reactance values are in pu on 100 MVA base, and all generators are equipped with governor and PSS

Table 5. Load data

Load	Load A	Load B	Load C
Bus NO.	9	5	7
Active power [MW]	125	90	100
Reactive power [MVAR]	50	30	35
Number of blocks	6	4	5